The Canadian Mineralogist
Vol. 46, pp. 151-162 (2008)
DOI: 10.3749/canmin.46.1.151

THE CRYSTAL CHEMISTRY OF Al-RICH AMPHIBOLES: SADANAGAITE AND POTASSIC-FERRISADANAGAITE

FRANK C. HAWTHORNE§

Department of Geological Sciences, University of Manitoba, Winnipeg, Manitoba R3T 2N2, Canada

GEORGE E. HARLOW

Department of Earth and Planetary Sciences, American Museum of Natural History, New York, N.Y. 10024-5192, USA

ABSTRACT

The crystal structures of magnesiosadanagaite (MS) from Mogok, Myanmar, monoclinic, *a* 9.857(2), *b* 17.899(4), *c* 5.318(1) Å, β 105.36(1)°, *V* 904.74(8) Å^3, *C*2/*m*, Z = 2, and potassic-ferrisadanagaite (FS) from the Ilmen alkaline massif, South Urals, Russia, *a* 9.9257(4), *b* 18.0917(7), *c* 5.3709(2) Å, β 105.19(1)°, *V* 930.75(2) Å^3, *C*2/*m*, Z = 2, have been refined to *R* values of ~3% using single-crystal Mo*K*α X-ray data. The crystals used in the collection of the intensity data were subsequently analyzed by electron-microprobe techniques, leading to the following compositions: MS: $(Na_{0.82}\ K_{0.17})\ (Ca_{1.95}\ Na_{0.05})\ (Mg_{3.36}\ Fe^{2+}_{0.23}\ Al_{1.20}\ Cr^{3+}_{0.07}\ Ti^{4+}_{0.16})\ (Si_{5.47}\ Al_{2.53})\ O_{22}\ [(OH)_{1.58}\ F_{0.42}]$; FS: $(Na_{0.31}\ K_{0.62})\ (Ca_{1.72}\ Na_{0.28})\ (Mg_{0.56}\ Fe^{2+}_{2.12}\ Mn^{2+}_{0.26}\ Zn_{0.02}\ Al_{0.72}\ Fe^{3+}_{1.07}\ Ti^{4+}_{0.21})\ (Si_{5.24}\ Al_{2.76})\ O_{22}\ [(OH)_{1.70}\ F_{0.30}]$. Site populations were assigned from the results of site-scattering refinement and stereochemical analysis, taking into account the unit formula determined for each crystal. The <*T*–O> distances, 1.678 and 1.684 Å, indicate that $^{[4]}$Al is strongly ordered at the *T*(1) site in each crystal, but the <*T*(2)–O> distances, 1.648 and 1.655 Å, indicate significant Al at the *T*(2) site. The Fe^{2+} and Fe^{3+} contents in each crystal were assigned from the <*M*–O> distances. The *A*(2) and *A*(*m*) sites are occupied by Na and (Na,K), respectively, in crystal MS, and by Na and K, respectively, in crystal FS. Both amphiboles show SRO (short-range order) of species at the *M*(4), O(3), *A*(*m*) and *A*(2) sites, and the relative abundances of these arrangements were assigned.

Keywords: amphibole, magnesiosadanagaite, potassic-ferrisadanagaite, crystal-structure refinement, electron-microprobe analysis, Mogok, Myanmar, Ilmen, South Urals, Russia.

SOMMAIRE

Nous avons affiné la structure cristalline de la magnésiosadanagaïte (MS) provenant de Mogok, Myanmar, monoclinique, *a* 9.857(2), *b* 17.899(4), *c* 5.318(1) Å, β 105.36(1)°, *V* 904.74(8) Å^3, *C*2/*m*, Z = 2, et de la potassic-ferrisadanagaïte (FS) provenant du massif alcalin d'Ilmen, secteur austral des Ourales, en Russie, *a* 9.9257(4), *b* 18.0917(7), *c* 5.3709(2) Å, β 105.19(1)°, *V* 930.75(2) Å^3, *C*2/*m*, Z = 2, jusqu'à un résidu d'environ 3% au moyen de données en diffraction X prélevées sur monocristal (rayonnement Mo*K*α). Les cristaux utilisés pour l'ébauche de la structure ont par la suite été analysés avec une microsonde électronique, ce qui a mené aux compositions: MS: $(Na_{0.82}\ K_{0.17})\ (Ca_{1.95}\ Na_{0.05})\ (Mg_{3.36}\ Fe^{2+}_{0.23}\ Al_{1.20}\ Cr^{3+}_{0.07}\ Ti^{4+}_{0.16})\ (Si_{5.47}\ Al_{2.53})\ O_{22}\ [(OH)_{1.58}\ F_{0.42}]$; FS: $(Na_{0.31}\ K_{0.62})\ (Ca_{1.72}\ Na_{0.28})\ (Mg_{0.56}\ Fe^{2+}_{2.12}\ Mn^{2+}_{0.26}\ Zn_{0.02}\ Al_{0.72}\ Fe^{3+}_{1.07}\ Ti^{4+}_{0.21})\ (Si_{5.24}\ Al_{2.76})\ O_{22}\ [(OH)_{1.70}\ F_{0.30}]$. La population des sites a été attribuée selon les résultats de la dispersion des électrons à chaque site et une analyse stéréochimique, compte tenu de la formule unitaire déterminée pour chaque cristal. Selon les distances <*T*–O> de 1.678 et 1.684 Å, $^{[4]}$Al serait fortement ordonné sur le site *T*(1) dans chaque cristal, mais les distances <*T*(2)–O>, égales à 1.648 et 1.655 Å, indiquent une proportion importante de Al au site *T*(2). Les teneurs de Fe^{2+} et Fe^{3+} ont été affinées selon les distances <*M*–O>. Les sites *A*(2) et *A*(*m*) sont occupés par Na et (Na,K), respectivement, dans le cristal MS, et par Na et K, respectivement, dans le cristal FS. Les deux amphiboles font preuve d'une mise en ordre à courte échelle impliquant les sites *M*(4), O(3), *A*(*m*) et *A*(2), et nous précisons la proportion de ces agencements.

(Traduit par la Rédaction)

Mots-clés: amphibole, magnésiosadanagaïte, potassic-ferrisadanagaïte, affinement de la structure cristalline, analyse à la microsonde électronique, Mogok, Myanmar, Ilmen, Ourales australes, Russie.

§ *E-mail address*: frank_hawthorne@umanitoba.ca

Introduction

The stereochemical characteristics of Al-rich amphiboles are still not very well resolved owing to the paucity of appropriate chemical compositions. Detailed studies by Leake (1968) and Robinson *et al.* (1982) show that amphiboles with $^{[4]}$Al (tetrahedrally coordinated Al) in excess of 2 *apfu* (atoms per formula unit) are uncommon, and that amphiboles with $^{[4]}$Al above 2.5 *apfu* are rare. Nevertheless, such amphiboles do occur (*e.g.*, Appleyard 1975, Hawthorne & Grundy 1977, Shimazaki *et al.* 1984, Mogessie *et al.* 1986, Sawaki 1989, Bazhenov *et al.* 1999, Banno *et al.* 2004) and are important for two reasons: (1) they "pin" the ends of mean bond-length – constituent ionic-radius relations, thereby making these relations both more accurate and more precise, and (2) extreme chemical compositions can expose new (or hitherto overlooked) mechanisms of substitution or ordering in the amphibole structure. To this end, we here refine the crystal structures of magnesiosadanagaite from Mogok, Myanmar, and potassic-ferrisadanagaite from the Ilmen alkaline massif, Ilmen mountains, southern Urals, Russia, and compare their stereochemistry with recently developed predictive curves (Hawthorne & Oberti 2007).

Review of our State of Knowledge

Early studies of aluminous amphiboles were done with two-dimensional diffraction data. The authors assumed disordered site-populations at the *T*(1) and *T*(2) sites in the *C*2/*m* amphibole structure (Heritsch & Kahler 1960, Heritsch & Reichert 1960, Heritsch *et al.* 1957, 1960, Trojer & Walitzi 1965). Papike *et al.* (1969) first showed that the <*T*(1)–O> distances are longer than the <*T*(2)–O> distances in $^{[4]}$Al-bearing amphiboles, and Hawthorne & Grundy (1973a, b) and Robinson *et al.* (1973) proposed relations between <*T*(1)–O> and <*T*(2)–O> distances and $^{[4]}$Al site-populations in *C*2/*m* amphiboles. Hawthorne & Grundy (1977) refined the structure of what is now named potassian ferri-ferrosadanagaite and showed that Al can occupy the *T*(2) site in significant amounts. Shimazaki *et al.* (1984) described sadanagaite and magnesiosadanagaite with $^{[4]}$Al < 2.50 *apfu* and $^{[4]}$Al = 3.48 *apfu*. The situation was slightly complicated by publication of a new nomenclature for amphiboles (Leake *et al.* 1997), in which the ideal compositions of sadanagaite and magnesiosadanagaite were redefined as ^{A}Na- dominant, with the result that the originally approved sadanagaite and magnesiosadanagaite became potassicsadanagaite and potassic magnesiosadanagaite. In turn, Banno *et al.* (2004) described magnesiosadanagaite as defined under the new (Leake *et al.* 1997) scheme of nomenclature. Oberti *et al.* (1995b) reconsidered the relations between <*T*(1)–O> and <*T*(2)–O> distances and $^{[4]}$Al site-populations in *C*2/*m* amphiboles and showed that the <*T*(2)–O> distance is affected by other compositional variations in the structure in addition to the $^{[4]}$Al site-population. Sokolova *et al.* (2000) refined the structure of potassic-ferrisadanagaite by the Rietveld method and used a slightly modified version of the curve of Oberti *et al.* (1995b) to assign $^{[4]}$Al site-populations. Furthermore, they noted that prediction for the potassian ferri-ferrosadanagaite of Hawthorne & Grundy (1977) results in an $^{[4]}$Al content that differs significantly from the chemical composition of the crystal. Banno *et al.* (2004) noted that the curve for *T*(2) given by Sokolova *et al.* (2000) does not predict sufficient Al at this site to agree with the chemical composition of the crystal. Oberti *et al.* (1995b) showed that the distribution of Al over the *T*(1) and *T*(2) sites is slightly dependent on temperature of crystallization. However, it is apparent from the discovery of fluorocannilloite, ideally $Ca\,Ca_2\,(Mg_4Al)\,(Si_5\,Al_3)\,O_{22}\,F_2$ (Hawthorne *et al.* 1996a), that composition is also an important issue in more $^{[4]}$Al-rich structures, as the presence of Ca at the *A* site strongly affects the pattern of order of Al over the *T*(1) and *T*(2) sites.

Experimental

Magnesiosadanagaite (MS) occurs as a somewhat corroded single prismatic crystal (Fig. 1), coated with phlogopite, in a piece of marble with a nearby (1 cm) corundum (var. ruby) crystal (specimen AMNH 107971) from the Dattaw mine, Mogok Stone Tract, Mandalay Division, Myanmar (Burma); no other minerals were detectable in the sample. Pargasite and edenite are the most common species of amphibole from the Mogok marbles, but Dattaw is noteworthy because it occurs at the intersection of a marble horizon and a pegmatite dike related to the Kabaing granite (Themelis 2007). Here, corundum in marble is commonly associated with cancrinite (blue), sodalite (colorless), nepheline, marialite, a tourmaline (foitite or burgerite?), apatite and phlogopite, which Harlow *et al.* (2006) and Themelis (2007) interpreted as products of a reaction between the pegmatite and marble (*i.e.,* skarn). These interactions may have played a role in the paragenesis of magnesiosadanagaite. The phlogopite overgrowth on the amphibole may well reflect the effect of the pegmatite. No other specimens of magnesiosadanagaite has been observed among "Mogok" specimens at the American Museum of Natural History (> 400 specimens).

Potassic-ferrisadanagaite (FS) occurs as a rock-forming mineral in an alkaline syenite in thin interrupted bands along the eastern contact of the Ilmen alkaline massif, southern Urals, Russia (Bazhenov *et al.* 1999). FS occurs with plagioclase ($An_{26–28}$), fine-grained perthitic alkali feldspar and grossular–andradite, with accessory apatite, titanite and allanite. In fine-grained rocks, FS forms short prismatic grains, whereas in coarse-grained pegmatitic rocks, FS forms

FIG. 1. Magnesiosadanagaite mantled by phlogopite (brown) adjacent to corundum (variety ruby) in white marble from the Dattaw mine, Mogok Stone Tract, Mandalay Division, Myanmar. The specimen measures 8.5 × 4.0 × 2.5 cm.

TABLE 1. MISCELLANEOUS INFORMATION FOR MAGNESIOSADANAGAITE (MS) AND POTASSIC-FERRISADANAGAITE (FS)

	MS	FS		MS	FS
a (Å)	9.857(2)	9.9257(4)	crystal size (mm)	0.08 x 0.10 x 0.16	0.05 x 0.11 x 0.11
b	17.899(4)	18.0917(7)	radiation/mono.	Mo*K*α/Graphite	Mo*K*α/Graphite
c	5.318(1)	5.3709(2)	no. of reflections	4216	4378
β (°)	105.36(1)	105.19(1)	no. of unique ¦*F*¦	1356	1397
V (Å^3)	904.74(8)	930.75(2)	no. of $\|F_{obs.}\|$	1092	1159
Space group	*C*2/*m*	*C*2/*m*	R_o (¦F_o¦ > 4σ*F*) %	3.0	2.6
Z	2	2	wR_2 (%)	6.8	5.4

poikilitic crystals up to 2 cm across. Results of a Rietveld refinement and a Mössbauer spectrum of FS were given by Sokolova *et al*. (2000).

X-ray data collection and structure refinement

Experimental details are as described by Tait *et al*. (2005). Unit-cell parameters, *R* indices and other information pertinent to data collection and refinement are given in Table 1. Difference-electron-density maps were calculated from the final structure-models with the *A*-site cations omitted from the calculation, and are shown in Figure 2. Details of the *A*-site configurations are shown in Figure 3. Site scattering was refined at the *A*(*m*) and *A*(2) sites, but with isotropic-displacement factors, there was an additional residual peak at another *A*(*m*) [= *A*(*m*)'] site in both structures. Thus two *A*(*m*) sites were identified, and the site scattering was refined at all three *A* sites with the isotropic-displacement factors constrained to be equal at these sites in order to damp the extreme correlations that would otherwise occur between refined *A*-site variables. Final coordinates and displacement parameters of all atoms are listed in Table 2, selected interatomic distances and angles are given in Table 3, and the refined site-scattering values are listed in Table 4. A table of structure factors is available from the Depository of Unpublished Data on the Mineralogical Association of Canada website [document Sadanagaite CM46_151].

Electron-microprobe analysis

The crystals used in the collection of the X-ray intensity data were subsequently mounted, polished and analyzed using a CAMECA SX100 electron microprobe in wavelength-dispersion mode. Beam conditions for

all elements were 15 kV, beam current of 20 nA, and a spot diameter of 1 μm. Counting times for all element peak and background determinations were 20 s and 10 s, respectively. The analytical data were reduced and corrected using the PAP method (Pouchou & Pichoir 1985). The crystals were analyzed with the following standards for *K* X-ray lines: albite (Na), orthoclase (K), diopside (Ca, Si), arfvedsonite (Fe), spessartine (Mn), forsterite (Mg), chromite (Cr), titanite (Ti), kyanite (Al) and fluororiebeckite (F). The chemical compositions (Table 5) are the average of 10 determinations taken uniformly over each crystal; no significant zoning was observed. The resulting composition of potassic-ferrisadanagaite is very close to that given by Bazhenov *et al*. (1999).

Calculation of unit formulae

Calculation of the unit formulae for these crystals is not straightforward. Both crystals contain significant $^{[6]}Ti^{4+}$ (~0.20 *apfu*; atoms per formula unit), and the way that the Ti is treated significantly affects the resultant formulae. Where $^{[6]}Ti^{4+}$ occurs in significant amounts (>0.2 *apfu*), it occurs at the *M*(1) site, entering the structure *via* the substitution $^{M(1)}Ti^{4+} + 2\ ^{O(3)}O^{2-} \rightleftharpoons {}^{M(1)}Mg + 2\ ^{O(3)}(OH)$ (Oberti *et al*. 1992, Hawthorne *et al*. 1998), thereby affecting the amount of OH in the structure and hence the normalization procedure in the absence of a determination for H. However, in the present case, we will see that the <*M*(1)–O> distances are not compatible with significant amounts of Ti at

TABLE 2. ATOM COORDINATES AND DISPLACEMENT PARAMETERS FOR MAGNESIOSADANAGAITE AND POTASSIC-FERRISADANAGAITE

	x	*y*	*z*	U_{11}	U_{22}	U_{33}	U_{23}	U_{13}	U_{12}	U_{eq}
					Magnesiosadanagaite					
O(1)	0.10412(19)	0.09060(9)	0.2124(3)	0.0102(10)	0.0167(9)	0.0097(9)	−0.0007(7)	0.0023(8)	−0.0029(7)	0.0122(6)
O(2)	0.11794(19)	0.17446(9)	0.7416(3)	0.0118(10)	0.0103(8)	0.0098(9)	0.0015(7)	0.0012(8)	0.0002(7)	0.0110(6)
O(3)	0.1085(3)	0	0.7135(5)	0.0150(15)	0.0152(13)	0.0140(14)	0	0.0031(11)	0	0.0149(9)
O(4)	0.3701(2)	0.25257(10)	0.7933(3)	0.0177(11)	0.0097(8)	0.0123(10)	0.0007(7)	0.0068(8)	0.0006(7)	0.0127(6)
O(5)	0.3522(2)	0.14183(10)	0.1177(4)	0.0122(10)	0.0139(9)	0.0127(9)	0.0031(7)	0.0013(8)	−0.0013(7)	0.0133(6)
O(6)	0.3420(2)	0.11722(9)	0.6127(4)	0.0116(10)	0.0146(9)	0.0145(10)	−0.0034(8)	0.0010(8)	0.0014(7)	0.0140(6)
O(7)	0.3370(3)	0	0.2753(5)	0.0164(16)	0.0151(13)	0.0192(14)	0	0.0067(13)	0	0.0165(9)
T(1)	0.27989(8)	0.08649(4)	0.30485(14)	0.0111(4)	0.0105(4)	0.0098(4)	−0.0001(3)	0.0020(3)	−0.0008(3)	0.0106(2)
T(2)	0.29138(8)	0.17420(4)	0.81875(13)	0.0102(4)	0.0091(3)	0.0084(4)	0.0005(3)	0.0021(3)	0.0001(3)	0.0093(2)
M(1)	0	0.08994(6)	1/2	0.0089(7)	0.0073(6)	0.0052(6)	0	0.0018(5)	0	0.0071(4)
M(2)	0	0.17641(5)	0	0.0053(6)	0.0054(5)	0.0049(6)	0	0.0012(4)	0	0.0052(4)
M(3)	0	0	0	0.0083(9)	0.0052(8)	0.0054(9)	0	0.0009(6)	0	0.0065(5)
M(4)	0	0.28115(4)	1/2	0.0122(4)	0.0091(4)	0.0100(4)	0	0.0039(3)	0	0.0103(3)
H(1)										
*A*2/m	0	1/2	0	0.05000(0)						
A(*m*)	0.017(5)	1/2	0.039(10)	0.0292(18)						
A(*m*)′	0.049(8)	1/2	0.106(16)	0.0292(18)						
A(2)	1/2	−0.0298(7)	0	0.0292(18)						
					Potassic-ferrisadanagaite					
O(1)	0.1029(2)	0.09398(11)	0.2099(4)	0.0118(9)	0.0139(9)	0.0113(10)	−0.0006(7)	0.0027(8)	−0.0005(8)	0.0124(4)
O(2)	0.1187(2)	0.17763(11)	0.7449(4)	0.0113(9)	0.0129(9)	0.0105(9)	0.0003(7)	0.0013(7)	0.0009(7)	0.0119(4)
O(3)	0.1101(3)	0	0.7106(6)	0.0113(14)	0.0156(14)	0.0129(14)	0	0.0028(11)	0	0.0133(6)
O(4)	0.3715(2)	0.25126(11)	0.7954(4)	0.0144(10)	0.0114(9)	0.0123(10)	−0.0002(8)	0.0056(8)	−0.0003(8)	0.0123(4)
O(5)	0.3518(2)	0.13948(11)	0.1136(4)	0.0113(9)	0.0147(9)	0.0121(10)	0.0029(8)	0.0024(8)	−0.0005(8)	0.0128(4)
O(6)	0.3406(2)	0.11902(11)	0.6082(4)	0.0117(10)	0.0147(10)	0.0149(10)	−0.0033(8)	0.0033(8)	0.0017(8)	0.0138(4)
O(7)	0.3300(3)	0	0.2878(6)	0.0158(15)	0.0140(14)	0.0225(16)	0	0.0041(13)	0	0.0176(6)
T(1)	0.27785(8)	0.08708(4)	0.30453(15)	0.0107(4)	0.0106(3)	0.0099(4)	−0.0002(3)	0.0020(3)	−0.0007(3)	0.01051(18)
T(2)	0.29168(8)	0.17379(4)	0.81893(15)	0.0094(4)	0.0093(3)	0.0075(3)	0.0001(3)	0.0020(3)	−0.0002(3)	0.00879(17)
M(1)	0	0.09139(4)	1/2	0.0082(3)	0.0081(3)	0.0042(3)	0	0.0026(2)	0	0.0066(2)
M(2)	0	0.17959(4)	0	0.0043(4)	0.0037(4)	0.0038(4)	0	0.0009(3)	0	0.0040(2)
M(3)	0	0	0	0.0075(5)	0.0044(4)	0.0045(4)	0	0.0008(3)	0	0.0056(3)
M(4)	0	0.28249(5)	1/2	0.0125(4)	0.0103(4)	0.0110(4)	0	0.0055(3)	0	0.0108(3)
H(1)	0.2106(13)	0	0.740(10)	0.01599(0)						
A	0	1/2	0	0.03000(0)						
A(*m*)	0.02223(0)	1/2	0.04661(0)	0.0177(12)						
A(*m*)′	0.065(3)	1/2	0.131(5)	0.0177(12)						
A(2)	0	0.4795(11)	0	0.0177(12)						

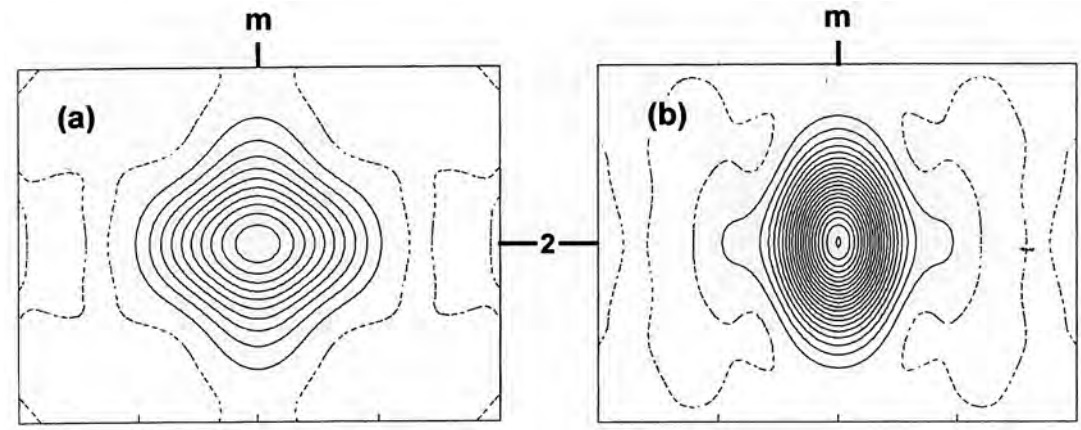

FIG. 2. Difference-Fourier maps for (a) magnesiosadanagaite and (b) potassic-ferrisadanagaite calculated with the *A*-site cations removed from the structural model; the maps are parallel to $(\bar{2}01)$, and the zero contour is dashed.

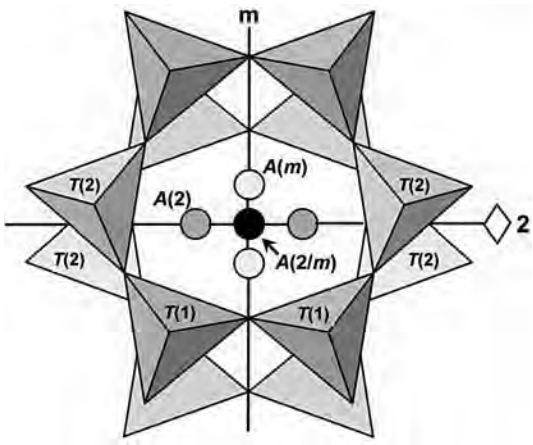

FIG. 3. The arrangement of polyhedra around the *A* cavity and the *A* sites in the *C*2/*m* amphibole structure; the *A*(*m*) and *A*(*m*)' sites overlap at the scale of this figure.

M(1), and hence we calculated the formulae on the basis of 24 anions *pfu* with (OH) + F = 2 *apfu*. For crystal MS, the observed <*M*(2)–O> distance and the mean bond-length – aggregate-cation-radius relation of Hawthorne (unpublished) indicate zero Fe^{3+} at the *M*(2) site, and hence zero Fe^{3+} in the structure. For crystal FS, the Fe^{3+} content was derived from the Mössbauer results of Sokolova *et al*. (2000). The resulting unit formulae are given in Table 5.

SITE POPULATIONS

The site populations were assigned on the basis of (1) the refined site-scattering values (Table 4), (2) the unit formulae derived from the chemical compositions determined by electron-microprobe analysis (Table 5), (3) the observed bond-lengths (Table 3), (4) the constraint that all sites except *A* be fully occupied, and (5) the resulting formula be neutral.

The T sites

The site populations at the *T*(1) and *T*(2) sites in these amphiboles are of significant interest, as the compositions reported here are some of the most $^{[4]}$Al-rich of the monoclinic amphiboles. Our current curves relating <*T*–O> distances and ^{T}Al content (Oberti *et al*. 1995b) do not work very well for Al-rich amphiboles.

Hawthorne & Oberti (2007) have reconsidered this problem in detail using data from ~50 refined amphiboles from the literature. The issue is complicated by the fact that the grand mean *T*–O distance, <<*T*–O>>, is not a simple linear function of the $^{[4]}$Al content over the complete range of $^{[4]}$Al values in amphiboles (Fig. 4a). At small values of $^{[4]}$Al (<0.50 *apfu*), there is significant variation in $^{[4]}$Al that appears unrelated to $^{[4]}$Al content, and Hawthorne & Oberti (2007) showed that the variation of <<*T*–O>> in Figure 4a is related to compositional variations in other parts of the structure in addition to the *T* sites. However, there is a linear relation between <<*T*–O>> and $^{[4]}$Al for $^{[4]}$Al >0.50 *apfu* (Fig. 4b), implying that there should be linear relations between both <*T*(1)–O> and $^{T(1)}$Al, and <*T*(2)–O> and $^{T(2)}$Al; Hawthorne & Oberti (2007) provided these relations (Figs. 4c, d): <*T*(1)–O> = 1.6202(6) + 0.0308(4) $^{T(1)}$Al, R = 0.996, σ = 0.0012 Å, $^{T(1)}$Al = –52.12 + 32.177 <(*T*(1)–O>, R = 0.996, σ = 0.039 Al *apfu*; <*T*(2)–O> = 1.6229(10) + 0.0329(3) $^{T(2)}$Al, R = 0.981, σ = 0.0012 Å, $^{T(2)}$Al = –47.613 + 29.228 <(*T*(1)–O>, R = 0.981, σ = 0.035 Al *apfu*. The site populations were initially

TABLE 3. SELECTED INTERATOMIC DISTANCES (Å) AND ANGLES (°) IN MAGNESIOSADANAGAITE FROM MOGOK, MYANMAR

		MS	FS			MS	FS
T(1)–O(1)		1.673(2)	1.681(2)	*T*(2)–O(2)		1.649(2)	1.660(2)
T(1)–O(5)		1.690(2)	1.698(2)	*T*(2)–O(4)		1.626(2)	1.631(2)
T(1)–O(6)		1.681(2)	1.688(2)	*T*(2)–O(5)		1.649(2)	1.659(2)
T(1)–O(7)		1.669(1)	1.668(1)	*T*(2)–O(6)		1.667(2)	1.669(2)
<*T*(1)–O>		1.678	1.684	<*T*(2)–O>		1.648	1.655
M(1)–O(1)	x2	2.055(2)	2.076(2)	*M*(3)–O(1)	x4	2.085(2)	2.145(2)
M(1)–O(2)	x2	2.121(2)	2.177(2)	*M*(3)–O(3)	x2	2.081(3)	2.122(3)
M(1)–O(3)	x2	2.093(2)	2.135(2)	<*M*(3)–O>		2.084	2.137
<*M*(1)–O>		2.090	2.129				
				M(4)–O(2)	x2	2.420(2)	2.430(2)
M(2)–O(1)	x2	2.018(2)	2.027(2)	*M*(4)–O(4)	x2	2.344(2)	2.362(2)
M(2)–O(2)	x2	2.022(2)	2.028(2)	*M*(4)–O(5)	x2	2.567(2)	2.620(2)
M(2)–O(4)	x2	1.928(2)	1.915(2)	*M*(4)–O(6)	x2	2.567(2)	2.549(3)
<*M*(2)–O>		1.989	1.990	<*M*(4)–O>		2.475	2.49
A–O(5)	x4	3.073(2)	3.062(2)	*A*(*m*)′–O(5)	x2	3.07(5)	3.039(2)
A–O(6)	x4	3.061(2)	3.134(2)	*A*(*m*)′–O(5)	x2	3.21(5)	3.111(2)
A–O(7)	x2	2.443(3)	2.570(4)	*A*(*m*)′–O(6)	x2	2.63(4)	2.933(2)
<*A*–O>		2.942	2.992	*A*(*m*)′–O(6)	x2	3.55(6)	3.348(2)
				A(*m*)′–O(7)		2.49(9)	2.572(2)
A(2)–O(5)	x2	2.649(10)	2.763(16)	*A*(*m*)′–O(7)		2.56(9)	2.600(3)
A(2)–O(5)	x2	3.527(11)	3.375(18)	*A*(*m*)′–O(7)		3.18(8)	3.490(3)
A(2)–O(6)	x2	2.723(7)	2.891(13)				
A(2)–O(6)	x2	3.449(10)	3.400(16)	*M*(1)–*M*(1)		3.220(2)	3.307(1)
A(2)–O(7)	x2	2.501(4)	2.597(5)	*M*(1)–*M*(2)		3.077(1)	3.124(1)
				M(1)–*M*(3)		3.108(1)	3.154(1)
A(*m*)–O(5)	x2	3.06(3)	3.057(12)	*M*(1)–*M*(4)		3.422(1)	3.457(1)
A(*m*)–O(5)	x2	3.10(3)	3.280(15)	*M*(2)–*M*(3)		3.158(1)	3.249(1)
A(*m*)–O(6)	x2	2.90(3)	2.604(16)	*M*(2)–*M*(4)		3.253(1)	3.268(1)
A(*m*)–O(7)		2.43(6)	2.68(2)				
A(*m*)–O(7)		2.48(6)	2.72(2)	*T*(1)–O(5)–*T*(2)		132.2(1)	132.9(1)
A(*m*)–O(7)		3.55(5)	3.02(3)	*T*(1)–O(6)–*T*(2)		138.2(1)	139.4(1)
				T(1)–O(7)–*T*(1)		136.1(2)	141.6(2)

calculated using these equations, and then adjusted to fit the total ^{T}Al from the unit formula.

As is apparent from Figures 4b–d, the data for magnesiosadanagaite and potassic-ferrisadanagaite are completely in accord with these relations, and confirm the fit for amphiboles with high (>2.00 Al *apfu*) ^{T}Al content. The data for the potassian ferri-ferrosadanagaite of Hawthorne & Grundy (1977) are the only other data so far available at these high ^{T}Al contents and are also in accord with the general relations of Figure 4. Note that in Figure 4c, there are three amphiboles that have higher Al contents at the *T*(1) site than these crystals of sadanagaite. These are samples of fluorocannilloite, in which the significant content of Ca at the *A*(2) site allows $^{T(1)}$Al to significantly exceed the value of 2.00 *apfu* by providing sufficient bond-valence at O(7) to compensate for the reduced bond-valence arising from the ensuing $^{T(1)}$Al–O(7)–$^{T(1)}$Al linkages (Hawthorne *et al.* 1996d).

The M(1,2,3) sites

Inspection of Table 5 shows that the *C*-group cations consist of Mg, Fe^{2+}, Mn^{2+}, Al, Fe^{3+}, Cr^{3+} and Ti^{4+}. Initially, we will assign Al, Fe^{3+}, Cr^{3+} and Ti^{4+} to *M*(2), treat Fe^{2+} and Mn^{2+} together (represented by the scattering factor for Fe), and derive the Mg and Fe site-populations from the refined site-scattering values

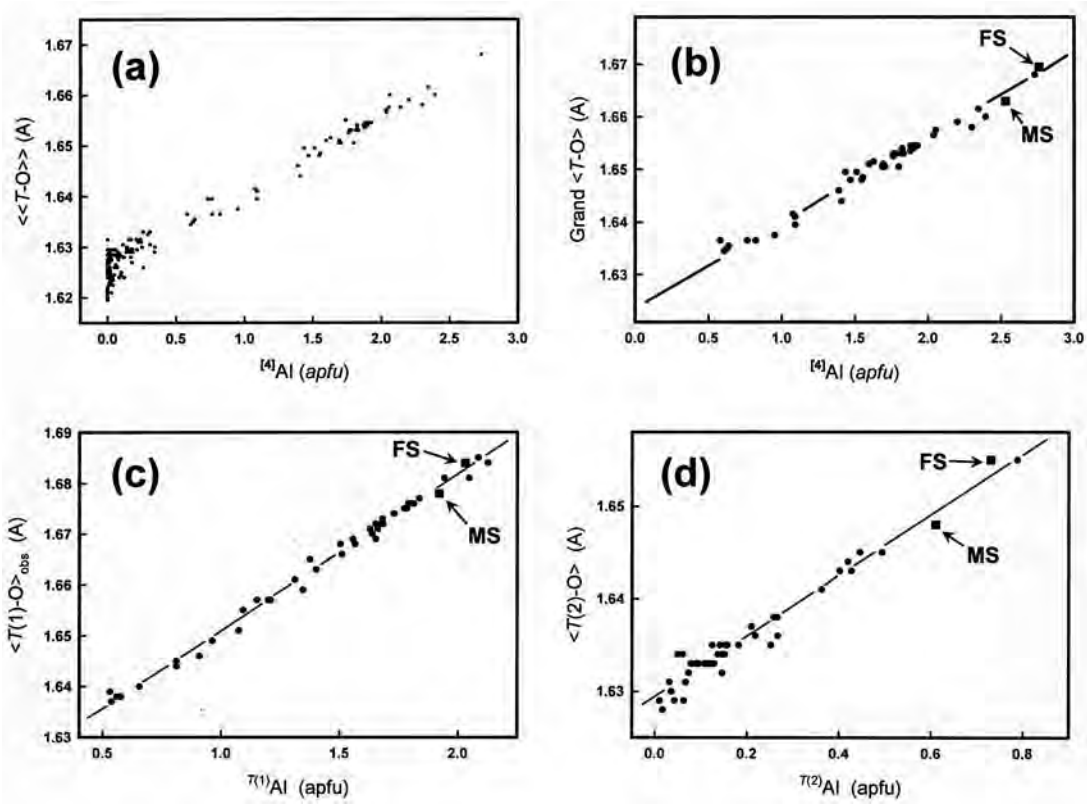

FIG. 4. Relations between *T*–O distance and [4]Al content in *C*2/*m* amphiboles; (a) <<*T*–O>> as a function of [4]Al; (b) <<*T*–O>> as a function of [4]Al (where [4]Al > 0.50 *apfu*); (c) <*T*(1)–O> as a function of $^{T(1)}$Al; (d) <*T*(2)–O> as a function of $^{T(2)}$Al. In (b), (c) and (d), the data for magnesiosadanagaite (MS) and potassic-ferrisadanagaite (KS) are shown by large black squares. Modified from Hawthorne & Oberti (2007).

TABLE 4. REFINED SITE-SCATTERING VALUES (*epfu*) FOR MAGNESIOSADANAGAITE AND POTASSIC-FERRISADANAGAITE

	MS		FS	
M(1)	24.8(1)	25.8*	46.7(2)	46.8*
M(2)	26.7(1)	27.7	38.7(2)	38.8
M(3)	12.80(8)	13.3	24.6(1)	24.6
Σ*M*(1,2,3)	64.3	66.8	110.0	110.2
C	66.8		110.2	
M(4)	39.0(1)		37.6(2)	
B	39.5		38.1	
A(2/*m*)	–		–	
A(2)	5.1(1)		3.5(2)	
A(*m*)′	2.2(1.0)		9.9(4)	
A(*m*)	4.9(1.1)		1.9(1)	
Σ*A* (SREF)	12.2		15.3	
A (EMPA)	12.1		15.9	

*These values are normalized to sum to the effective scattering of the *C*-group cations in the unit formulae.

TABLE 5. CHEMICAL COMPOSITION AND UNIT FORMULA OF MAGNESIOSADANAGAITE (MS) AND POTASSIC-FERRISADANAGAITE (FS)

	MS	FS		MS	FS
SiO_2 wt.%	38.42	33.02	Si *apfu*	5.47	5.24
Al_2O_3	22.20	18.61	Al	2.53	2.76
TiO_2	1.48	1.78	Σ*T*	8.00	8.00
Cr_2O_3	0.60	0.00			
Fe_2O_3	0.00	8.95	Al	1.20	0.72
FeO	1.92	15.96	Fe^{3+}	–	1.07
MnO	0.00	1.92	Ti^{4+}	0.16	0.21
ZnO	0.00	0.19	Fe^{2+}	0.23	2.12
MgO	15.81	2.35	Mn	–	0.26
CaO	12.77	10.09	Cr	0.07	–
Na_2O	3.14	1.91	Zn	–	0.02
K_2O	0.92	3.04	Mg	3.36	0.56
F	0.94	0.60	Σ*C*	5.02	4.96
(H_2O)	1.66	1.60			
O≡F	–0.40	–0.25	Ca	1.95	1.72
			Na	0.05	0.28
Sum	99.46	99.77	Σ*B*	2.00	2.00
			Na	0.82	0.31
			K	0.17	0.62
			Σ*A*	0.99	0.93
			OH	1.58	1.70
			F	0.42	0.30

(Table 4). The agreement between the total scattering at the *M*(1,2,3) sites and the aggregate number of electrons of the *C*-group cations is quite close, but we are still left with the problem that the numbers do not agree *exactly*, and hence any assignment of site populations cannot agree exactly with both sets of data. Site-scattering refinement determines the relative values of the individual site-scattering factors much more accurately than it determines the absolute values. This behavior arises because the refined scattering of the cations is determined relative to the scattering of the fixed cations and anions in the refinement procedure, and hence is dependent on the details of the scattering factors used (*i.e.*, ionized *versus* half-ionized *versus* neutral). This issue suggests that we should use the relative values of the site-scattering values, but normalize the sum of the absolute values to the number of aggregate electrons of the *C*-group cations. These normalized values are given in Table 6. Site populations involving Mg and Fe^{2+} at *M*(1) and *M*(3) were calculated directly from the normalized site-scattering values. All Al, Cr^{3+} and Ti^{4+} were assigned to *M*(2), and the balance of the site scattering was used to calculate the amounts of Mg and Fe at *M*(2). There is no Fe at *M*(2) in crystal MS, and so we calculated the final formula with all Fe as Fe^{2+}. For crystal FS, the value of Fe^{3+} / (Fe^{2+} + Fe^{3+}) derived from the SREF site-population is 0.335, in close agreement with the value of 0.32 derived by Mössbauer spectroscopy on the same sample (Sokolova *et al*. 2000).

Hawthorne & Oberti (2007) reported relations between <*M*–O> distances and mean constituent-cation and constituent-anion radii at the relevant sites. Using these relations, we may calculate <*M*–O> distances for proposed site-assignments and evaluate their validity from the correspondence between the observed and calculated <*M*–O> distances. There is no indication of Fe^{3+} at the *M*(1) and *M*(3) sites in crystal FS from the <*M*(1)–O> and <*M*(3)–O> distances, in accord with the agreement between the Fe^{3+} / (Fe^{2+} + Fe^{3+}) values determined by SREF and by Mössbauer spectroscopy (Sokolova *et al*. 2000). Is there significant Ti^{4+} at the *M*(1) site in these crystals? The calculated <*M*(1)–O> distances for (1) Ti^{4+} assigned to *M*(1) and (2) Ti^{4+} assigned to *M*(2) are (1) 2.076 and 2.108, and (2) 2.082 and 2.119 Å for MS and FS, respectively. The differences between the observed and calculated distances are twice as large for case (1) as for case (2), and hence we conclude that there is no significant Ti^{4+} at *M*(1) in either crystal.

There is significant Mn^{2+} in crystal FS; can we derive any information on the site occupancy of this cation? First, the calculated <*M*(2)–O> distance, 1.990 Å, is identical to the observed value, 1.990 Å, and the assigned site-populations are conformable with the observed mean bond-length without any Mn^{2+} at *M*(2), indicating that Mn^{2+} must occur at the *M*(1) or *M*(3) sites (or both). As Mn^{2+} (r = 0.83 Å; Shannon 1976) is significantly larger than Fe^{2+}, the presence of Mn^{2+} at a site should affect the mean bond-length. With the heavy scatterer at *M*(1) and *M*(3) assigned as Fe^{2+}, the calculated <*M*(1)–O> and <*M*(3)–O> distances are 2.119 and 2.122 Å, respectively, and the observed <*M*(1)–O> and <*M*(3)–O> distances are 2.129 and 2.137 Å. The differences are 0.010 and 0.015 Å, respectively. We may assign Mn^{2+} so as to minimize these differences: $^{M(1)}Mn^{2+}$ = 0.08, $^{M(3)}Mn^{2+}$ = 0.18 *apfu*. The resultant site-populations are given in Table 6.

TABLE 6. ASSIGNED SITE-POPULATIONS (*apfu*) IN MAGNESIOSADANAGAITE AND POTASSIC-FERRISADANAGAITE

Site	Species	Site populations		Site	Species	Site populations	
		MS	FS			MS	FS
T(1)	Si	2.06	1.88	*M*(3)	Mg	0.91	0.10
	Al	1.94	2.12		Fe^{2+}	0.09	0.72
	Σ	4.00	4.00		Mn	–	0.18
					Σ	1.00	1.00
T(2)	Si	3.44	3.22				
	Al	0.56	0.78	*M*(4)	Ca	1.95	1.72
	Σ	4.00	4.00		Na	0.05	0.28
					Σ	2.00	2.00
M(2)	Al	1.20	0.72				
	Fe^{3+}	–	0.84	*A*(*m*)′	K	0.12	0.52
	Ti	0.16	0.21				
	Cr	0.07	–	*A*(*m*)	K	0.05	0.10
	Zn	–	0.02		Na	0.36	–
	Mg	0.57	0.21				
	Σ	2.00	2.00	*A*(2)	Na	0.46	0.32
					Σ	0.99	0.94
M(1)	Mg	1.87	0.37				
	Fe^{2+}	0.13	1.55	*A*(2/*m*)	Na	–	–
	Mn	–	0.08		K	–	–
	Σ	2.00	2.00				

Units: atoms per formula unit (*apfu*). MS: magnesiosadanagaite; FS: potassic-ferrisadanagaite.

The M(4) site

The chemical compositions of Table 5 indicate that the *M*(4) site is dominated by Ca in these crystals, with the balance being made up of Na. The resultant site-populations are in close accord with the refined site-scattering values at this site (Table 6).

The A site

The *A* site is completely filled by Na and K in these amphiboles, and the refined site-scattering values are in accord with the chemical compositions given in Table 5. In the monoclinic amphiboles, there is significant positional disorder of Na and K within the *A* cavity, the cations occupying the *A*(*m*) and *A*(2) sites (Papike *et al*. 1969, Hawthorne & Grundy 1972, Hawthorne 1983, Hawthorne *et al*. 1996d). This issue is examined for the structures refined here in Figure 2, which shows difference-Fourier maps calculated with the *A*-site cations removed from the refinement model. In crystal MS (Fig. 2a, Table 6), the electron density is distributed approximately equally between the aggregate *A*(*m*) and *A*(2) sites (Fig. 3), whereas in crystal FS (Fig. 2b), the

electron density is much higher at the *A*(*m*) site relative to the *A*(2) site; these results are in good accord with the refined site-scattering at these sites (Table 6).

Both crystals show the presence of two distinct *A* sites on the mirror plane, *A*(*m*) and *A*(*m*)'. Hawthorne *et al*. (1996d) showed that in fluoro-amphiboles, the *A*(*m*) site is further displaced from the center of the *A* cavity than in hydroxy amphiboles. It is notable that both MS and FS contain significant amounts of F (Table 5), and we propose that the *A*(*m*)' site is locally associated with F at O(3), whereas the *A*(*m*) site is locally associated with (OH) at O(3).

Short-Range Order

Heritsch (1955) first showed that the *A* cations in monoclinic amphiboles are disordered off the central *A*(2/*m*) site (Fig. 3). This was confirmed in many subsequent studies (Gibbs 1966, Papike *et al*. (1969), Hawthorne & Grundy 1972, 1973a, b, Robinson *et al*. 1973). It was soon realized that K occupies the *A*(*m*) site only, whereas Na occurs at both the *A*(2) and *A*(*m*) sites. However, the reason(s) for this behavior proved elusive for many years. Eventually, Hawthorne *et al*. (1996c) showed that this behavior is related to short-range order (SRO) in the vicinity of the *A* site and the resulting bond-valence requirements of the *local* atomic arrangements. In addition, they listed the local atomic arrangements in the vicinity of the *A* site in order of favorability with regard to bond-valence requirements [Table 7; note that we have changed the order of the sites relative to that given by Hawthorne *et al*. (1996c), *i.e*., *M*(4)–*A*–O(3) rather than *M*(4)–O(3)–*A*]. Thus in Table 7, arrangement [1] is the most favorable from bond-valence perspective [*i.e*., the local agreement with the valence-sum rule (Brown 1981, 2002, Hawthorne 1997) is maximized], and hence this arrangement will occur in preference to any other, provided the chemical composition of the crystal is compatible with its existence. Arrangement [2] is second most favorable, and will occur where there is no $^{M(4)}$Na, $^{O(3)}$F or $^{A(m)}$Na available to form arrangement [1].

In previous considerations of SRO in the vicinity of the *A* site (Hawthorne *et al*. 1996c, 2000a, b, 2006, Tait *et al*. 2005), we did not explicitly consider one issue involving the local stoichiometry of the optimal clusters listed in Table 7. This consideration may be seen by referring to Figure 5. The *A*(2) site is adjacent to two O(3) sites (Fig. 5a), and where *A*(2) is occupied

TABLE 7. MOLE FRACTIONS OF LOCAL ARRANGEMENTS INVOLVING *A*- AND *B*-CATIONS AND *W* ANIONS

M(4)–*A**–O(3)		MS**	FS**
[1]	Na – $^{A(m)}$Na – F	0.025	–
[2]	Ca – $^{A(2)}$Na – OH	0.460	0.320
[3]	Na – $^{A(m)}$Na – OH	–	–
[4]	Ca – $^{A(m)}$Na – F	0.335	–
[5]	Ca – $^{A(2)}$Na – F	–	–
	Na – K – F	–	0.140
	Ca – K – F	–	0.160
	Ca – K – OH	0.170	0.320
	Ca – □ – OH	0.010	0.060

* [1] → [5] in order of decreasing favorability, after Hawthorne *et al*. (1996c);
** fraction of each arrangement in amphiboles MS and FS.

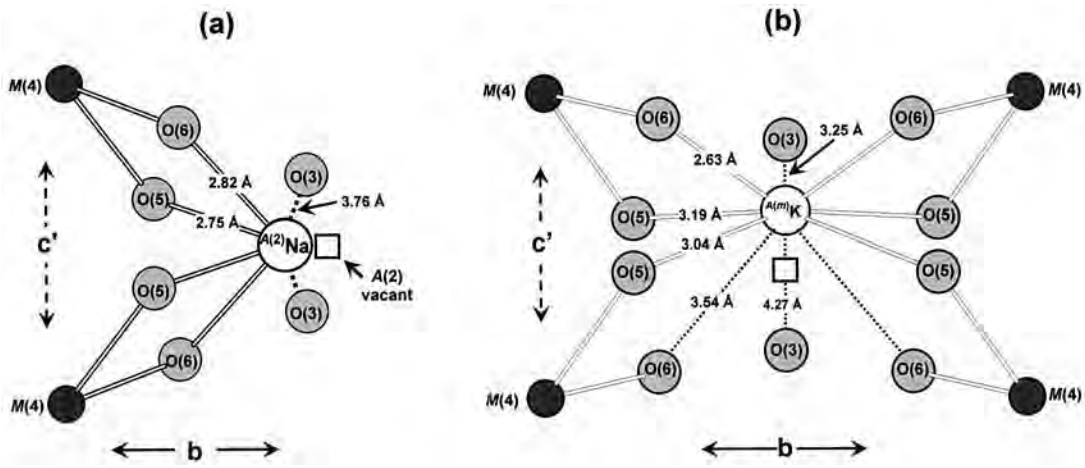

FIG. 5. The *C*2/*m* amphibole structure in the vicinity of the *A* site: short-range order of cations at the *A*(2) and *A*(*m*) sites: (a) $M(4)_2$–*A*(2)...$O(3)_2$, view rotated 10° from (100) to obviate overlap; the c' direction is dashed to indicate that it is inclined to the plane of the page; (b) $M(4)_2$–*A*(*m*)...O(3), view rotated 20° from (100). Symbols: *M*(4): black circles; *A*(2) and *A*(*m*): where occupied, large white circle, where not occupied, white square; the anions are large grey circles. Dotted lines indicate non-bonding distances.

by Na, there will be two $M(4)$ cations and two O(3) anions locally associated with this configuration of sites. Of course, this configuration is also associated with a vacant $A(2)$ site (Fig. 4a), but this does not affect the chemical composition of the local cluster, and we may omit it from the local configuration. Thus we may write the local configuration of occupied sites as follows: $M(4)_2$–$A(2)$–$O(3)_2$, where the subscript 2 indicates that two occupied sites occur in this configuration. The $A(m)$ site is adjacent to only one O(3) site (Fig. 5b), and hence where the $A(m)$ site is occupied by Na or K, there will be one O(3) anion locally associated with this arrangement. However, where one $A(m)$ site is locally occupied, all other locally associated A sites (compare Figs. 3 and 5b) are vacant, and the other O(3) site is locally associated with a vacant $A(m)$ site. We may write this local configuration as follows: $M(4)_2$–$A(m)$–O(3) + $O(3)^n$, where the superscript n indicates that the anion at this site is not specified [*i.e.*, it could be (OH) or F].

We may assign the arrangements listed in Table 7 to the refined structures MS and FS, beginning with the most strongly preferred arrangement: [1] $^{M(4)}$Na–$^{A(m)}$Na–$^{O(3)}$F. We will discuss the assignment for crystal MS such that the process (hopefully) becomes transparent; in essence, arrangements are assigned in decreasing order of favorability as cation and anion occupancies permit. There is 0.05 $^{M(4)}$Na present (Table 5), and hence the fraction of arrangement [1] present is 0.025. Arrangement [2] is limited by the amount of $^{A(2)}$Na: 0.46. Arrangement [3] cannot occur, as there is no $^{M(4)}$Na left from arrangement [1]. Arrangement [4] is limited by the amount of $^{A(m)}$Na remaining after formation of arrangement [1]: 0.335. Arrangement [5] cannot occur as there is no $^{A(2)}$Na left from arrangement [2]. The arrangement $^{M(4)}$Ca–$^{A(m)}$K–OH is dictated by the amount of K present: 0.17 (Table 5). This leaves 0.01 $^{A}\square$, which may occur as the cluster $^{M(4)}$Ca–$^{A}\square$–OH. The sum of the SRO arrangements is equal to the unit formula of the crystal (Table 5); the results for crystals MS and FS are given in Table 7.

This work, together with that of Hawthorne *et al.* (2000a, b, 2006) and Tait *et al.* (2005), show that there is strong SRO of cations and anions involving the A, $M(4)$ and O(3) sites. However, Hawthorne *et al.* (1996b, 2000b), Della Ventura *et al.* (1996, 1998, 1999, 2003) and Oberti *et al.* (1995a) have shown that there is extensive SRO of cations and anions involving the $M(1)$, $M(2)$, $M(3)$ and $T(1)$ sites. Presumably, the patterns of SRO over these two sets of sites are not independent, as the O(3) site is involved in both configurations of sites. Hence the next issue in our understanding of SRO in amphiboles is to establish what is the relation between these two types of SRO in different regions of the structure. This is not a straightforward matter, as (1) the optimum amphibole compositional system to do this needs to be identified, and (2) the coupling between these two short-range arrangements needs to be established.

Summary

(1) The crystal structures of magnesiosadanagaite and potassic-ferrisadanagaite, two of the three most $^{[4]}$Al-rich clino-amphiboles so far refined, are reported here.

(2) The grand <T–O> bond-lengths and analyzed amounts of $^{[4]}$Al are in accord with the relation between grand <T–O> and $^{[4]}$Al given by Hawthorne & Oberti (2007).

(3) The relation between <$M(1)$–O> and constituent-cation and constituent-anion radii (Hawthorne & Oberti 2007) indicates that Ti^{4+} is strongly to completely ordered at the $M(2)$ site.

(4) The A sites are occupied by both K and Na in both amphiboles. The $A(2)$ site is occupied by Na. There are two $A(m)$ sites: most of the K occurs at $A(m)'$, and small amounts of K ± Na occur at $A(m)$.

(5) On the basis of short-range bond-valence considerations (Hawthorne *et al.* 1996c), we show that there is strong short-range order of cations and anions involving the A, $M(4)$ and O(3) sites.

Acknowledgements

We thank Peter Robinson, an anonymous reviewer, Associate Editor Charles Geiger and Editor Bob Martin for their pertinent comments on this paper. FCH was supported by a Canada Research Chair in Crystallography and Mineralogy, by Major Equipment, Research Tools and Equipment, Discovery and Major Facilities Access grants from the Natural Sciences and Engineering Research Council of Canada, and by Innovation Grants from the Canada Foundation for Innovation.

References

Appleyard, E.C. (1975): Silica-poor hastingsitic ampiboles from the metasomatic alkaline gneisses at Wolfe, eastern Ontario. *Can. Mineral.* **13**, 342-351.

Banno, Y., Miyawaki, R., Matsubara, S., Makino, K., Bunno, M., Yamada, S. & Kamiya, T. (2004): Magnesiosadanagaite, a new member of the amphibole group from Kasuga-mura, Gifu prefecture, central Japan. *Eur. J. Mineral.* **16**, 177-183.

Bazhenov, A.G., Bazhenova, L.F., Krinova, T.V. & Khvorov, P.V. (1999): Potassicferrisadanagaite (K,Na) $Ca_2(Fe^{2+},Mg)_3(Fe^{3+},Al)_2[Si_5Al_3O_{22}](OH)_2$, a new mineral of the amphibole group (Ilmen Mountains, southern Urals). *Zap. Vser. Mineral. Obschchest.* **128**(4), 50-55 (in Russ.).

Brown, I.D. (1981): The bond valence method. An empirical approach to chemical structure and bonding. *In* Structure and Bonding in Crystals II (M. O'Keeffe & A. Navrotsky, eds.). Academic Press, New York, N.Y. (1-30).

BROWN, I.D. (2002): *The Chemical Bond in Inorganic Chemistry. The Bond Valence Model*. Oxford University Press, Oxford, U.K.

DELLA VENTURA, G., HAWTHORNE, F.C., ROBERT, J.-L., DELBOVE, F., WELCH, M.F. & RAUDSEPP, M. (1999): Short-range order of cations in synthetic amphiboles along the richterite–pargasite join. *Eur. J. Mineral.* **11**, 79-94.

DELLA VENTURA, G., HAWTHORNE, F.C., ROBERT, J.-L. & IEZZI, G. (2003): Synthesis and infrared spectroscopy of amphiboles along the tremolite–pargasite join. *Eur. J. Mineral.* **15**, 341-347.

DELLA VENTURA, G., ROBERT, J.-L. & HAWTHORNE, F.C. (1996): Infrared spectroscopy of synthetic (Ni,Mg,Co)-potassium-richterite. *In* Mineral Spectroscopy: A Tribute to Roger G. Burns (M.D. Dyar, C. McCammon & M.W. Schaefer, eds.). *Geochem. Soc., Spec. Publ.* **5**, 55-63.

DELLA VENTURA, G., ROBERT, J.-L. & HAWTHORNE, F.C. (1998): Characterization of OH–F short-range order in potassium-fluor-richterite by infrared spectroscopy in the OH-stretching region. *Can. Mineral.* **36**, 181-185.

GIBBS, G.V. (1966): Untitled article. *In* AGI Short Course Notes on Chain Silicates, 1-23.

HARLOW, G.E., PAMUKCU, A. & SAW NAUNG, K.T. (2006): Mineral assemblages and the origin of ruby in the Mogok Stone Tract, Myanmar. *Gems & Gemology* **42**, 147 (abstr.).

HAWTHORNE, F.C. (1983): The crystal chemistry of the amphiboles. *Can. Mineral.* **21**, 173-480.

HAWTHORNE, F.C. (1997): Short-range order in amphiboles: a bond-valence approach. *Can. Mineral.* **35**, 203-218.

HAWTHORNE, F.C., COOPER, M.A., GRICE, J.D. & OTTOLINI, L. (2000a): A new anhydrous amphibole from the Eifel region, Germany: description and crystal structure of obertiite, $NaNa_2(Mg_3Fe^{3+}Ti^{4+})Si_8O_{22}O_2$. *Am. Mineral.* **83**, 236-241.

HAWTHORNE, F.C., DELLA VENTURA, G. & ROBERT, J.-L. (1996a): Short-range order of (Na,K) and Al in tremolite: an infrared study. *Am. Mineral.* **81**, 782-784.

HAWTHORNE, F.C., DELLA VENTURA, G. & ROBERT, J.-L. (1996b): Short-range order and long-range order in amphiboles: a model for the interpretation of infrared spectra in the principal OH-stretching region. *In* Mineral Spectroscopy: A Tribute to Roger G. Burns (M.D. Dyar, C. McCammon & M.W. Schaefer, eds.). *Geochem. Soc., Spec. Publ.* **5**, 49-54.

HAWTHORNE, F.C. & GRUNDY, H.D. (1972): Positional disorder in the *A*-site of clino-amphiboles. *Nature* **235**, 72.

HAWTHORNE, F.C. & GRUNDY, H.D. (1973a): The crystal chemistry of the amphiboles. I. Refinement of the crystal structure of ferrotschermakite. *Mineral. Mag.* **39**, 36-48.

HAWTHORNE, F.C. & GRUNDY, H.D. (1973b): The crystal chemistry of the amphiboles. II. Refinement of the crystal structure of oxy-kaersutite. *Mineral. Mag.* **39**, 390-400.

HAWTHORNE, F.C. & GRUNDY, H.D. (1977): The crystal chemistry of the amphiboles. III. Refinement of the crystal structure of a sub-silicic hastingsite. *Mineral. Mag.* **41**, 43-50.

HAWTHORNE, F.C. & OBERTI, R. (2007): Amphiboles: crystal chemistry. *In* Amphiboles: Crystal Chemistry, Occurrence, and Health Issues (F.C. Hawthorne, R. Oberti, G. Della Ventura & A. Mottana, eds.). *Rev. Mineral. Geochem.* **67**, 1-54.

HAWTHORNE, F.C., OBERTI, R. & MARTIN, R.F. (2006): Short-range order in amphiboles from the Bear Lake Diggings, Ontario. *Can. Mineral.* **44**, 1171-1179.

HAWTHORNE, F.C., OBERTI, R. & SARDONE, N. (1996c): Sodium at the A site in clinoamphiboles: the effects of composition on patterns of order. *Can. Mineral.* **34**, 577-593.

HAWTHORNE, F.C., OBERTI, R., UNGARETTI, L. & GRICE, J.D. (1996d): A new hyper-calcic amphibole with Ca at the A site: fluor-cannilloite from Pargas, Finland. *Am. Mineral.* **81**, 995-1002.

HAWTHORNE, F.C., OBERTI, R., ZANETTI, A. & CZAMANSKE, G.K. (1998): The role of Ti in hydrogen-deficient amphiboles: sodic-calcic and sodic amphiboles from Coyote Peak, California. *Can. Mineral.* **36**, 1253-1265.

HAWTHORNE, F.C., WELCH, M.D., DELLA VENTURA, G., LIU, SHUANGXI, ROBERT, J.-L. & JENKINS, D.M. (2000b): Short-range order in synthetic aluminous tremolites: an infrared and triple-quantum MAS NMR study. *Am. Mineral.* **85**, 1716-1724.

HERITSCH, H. (1955): Bemerkungen zur Schreibung der kristallchemischen Formel der Hornblende. *Tschermaks Mineral. Petrogr. Mitt.* **5**, 242-245.

HERITSCH, H., BERTOLDI, G. & WALITZI, E.-M. (1960): Strukturuntersuchung an einer basaltischen Hornblende vom Kuruzzenkogel, südlich Fehring, Steiermark. *Tschermaks Mineral. Petrogr. Mitt.* **7**, 210-217.

HERITSCH, H. & KAHLER, E. (1960): Strukturuntersuchung an zwei Kluftkarinthinen, ein Beitrag zur Karinthinfrage. *Tschermaks Mineral. Petrogr. Mitt.* **7**, 218-234.

HERITSCH, H., PAULITSCH, P. & WALITIZI, E.-M. (1957): Die Struktur von Karinthin und einer barroisitischen Hornblende. *Tschermaks Mineral. Petrogr. Mitt.* **6**, 215-225.

HERITSCH, H. & REICHERT, L. (1960): Strukturuntersuchung an einer basaltischen Hornblende von Černošin, ČSR. *Tschermaks Mineral. Petrogr. Mitt.* **7**, 235-245.

LEAKE, B.E. (1968): A catalog of analyzed calciferous and subcalciferous amphiboles together with their nomenclature and associated minerals. *Geol. Soc. Am., Spec. Pap.* **98**.

LEAKE, B.E., WOOLLEY, A.R., ARPS, C.E.S., BIRCH, W.D., GILBERT, M.C., GRICE, J.D., HAWTHORNE, F.C., KATO, A., KISCH, H.J., KRIVOVICHEV, V.G., LINTHOUT, K., LAIRD, J., MANDARINO, J.A., MARESCH, W.V., NICKEL, E.H., ROCK, N.M.S., SCHUMACHER, J.C., SMITH, D.C., STEPHENSON, N.C.N., UNGARETTI, L., WHITTAKER, E.J.W. & GUO, YOUSHI (1997): Nomenclature of amphiboles: Report of the Subcommittee on Amphiboles of the International Mineralogical Association, Commission on New Minerals and Mineral Names. *Can. Mineral.* **35**, 219–246.

MOGESSIE, A., PURTSCHELLER, F. & TESSADRI, R. (1986): High alumina calcic amphiboles (alumino pargasite-magnesio sadanagaite) from metabasites and metacarbonates of central Oetztal, Eastern Alps (northern Tyrol, Austria). *Neues Jahrb. Mineral. Abh.* **154**, 21-39.

OBERTI, R., HAWTHORNE, F.C., UNGARETTI, L. & CANNILLO, E. (1995a): $^{[6]}$Al disorder in amphiboles from mantle peridotites. *Can. Mineral.* **33**, 867-878.

OBERTI, R., UNGARETTI, L., CANNILLO, E. & HAWTHORNE, F.C. (1992): The behaviour of Ti in amphiboles. I. Four- and six-coordinate Ti in richterite. *Eur. J. Mineral.* **3**, 425-439.

OBERTI, R., UNGARETTI, L., CANNILLO, E. & HAWTHORNE, F.C. & MEMMI, I. (1995b): Temperature-dependent Al order–disorder in the tetrahedral double-chain of *C*2/*m* amphiboles. *Eur. J. Mineral.* **7**, 1049-1063.

PAPIKE, J.J., ROSS, M. & CLARK, J.R. (1969): Crystal-chemical characterization of clinoamphiboles based on five new structure refinements. *Mineral. Soc. Am., Spec. Pap.* **2**, 117-136.

POUCHOU, J.L. & PICHOIR, F. (1985): "PAP" $\phi(\rho Z)$ procedure for improved quantitative microanalysis. *Microbeam Anal.*, 104-106.

ROBINSON, K., GIBBS, G.V., RIBBE, P.H. & HALL, M.R. (1973): Cation distribution in three hornblendes. *Am. J. Sci.* **273A**, 522-535.

ROBINSON, P., SPEAR, F.S., SCHUMACHER, J.C., LAIRD, J., KLEIN, C., EVANS, B.W. & DOOLAN, B.L. (1982): Phase relations of metamorphic amphiboles: natural occurrence and theory. *In* Amphiboles: Petrology and Experimental Phase Relations (D.R. Veblen & P.H. Ribbe, eds.). *Rev. Mineral.* **9B**, 1-227.

SAWAKI, T. (1989): Sadanagaite and subsilicic ferroan pargasite from thermally metamorphosed rocks in the Nōgō-Hakusan area, central Japan. *Mineral. Mag.* **53**, 99-106.

SHANNON, R.D. (1976): Revised effective ionic radii and systematic studies of interatomic distances in halides and chalcogenides. *Acta Crystallogr.* **A32**, 751-767.

SHIMAZAKI, H., BUNNO, M. & OZAWA, T. (1984): Sadanagaite and magnesio-sadanagaite, new silica-poor members of calcic amphibole from Japan. *Am. Mineral.* **69**, 465-471.

SOKOLOVA, E.V., HAWTHORNE, F.C., KABALOV, Y.K., SCHNEIDER, J. & MCCAMMON, C. (2000): The crystal chemistry of potassic-ferrisadanagaite. *Can. Mineral.* **38**, 669-674.

TAIT, K.T., HAWTHORNE, F.C., GRICE, J.D., OTTOLINI, L. & NAYAK, V.K. (2005): Dellaventuraite, $NaNa_2(MgMn^{3+}{}_2Ti^{4+}Li)Si_8O_{22}O_2$, a new anhydrous amphibole from the Kajlidongri manganese mine, Jhabua District, Madhya Pradesh, India. *Am. Mineral.* **90**, 304-309.

THEMELIS, T. (2007): *Gems and Mines of Mogôk: The Forbidden Land.* A & T, Los Angeles, California.

TROJER, F. & WALITIZI, E.-M. (1965): Strukturuntersuchung an einer Hornblende aus dem eklogitischen Gestein von Stramez, sudliche Koralpe. *Tschermaks Mineral. Petrogr. Mitt.* **10**, 233-240.

Received June 7, 2007, revised manuscript accepted January 29, 2008.